Atomization of cryogenic rocket engines coaxial injectors. Modeling aspects and experimental investigations

A. Murrone, N. Fdida, C. Le Touze, L. Vingert

Atomization of cryogenic rocket engines coaxial injectors. Modeling aspects and experimental investigations.

A. MURRONE*, N. FDIDA,
C. LE TOUZE, L. VINGERT
ONERA, The French Aerospace Lab
Chemin de la Hunière BP 80100
91123 Palaiseau Cedex
*author : murrone@onera.fr

Abstract
Even if it has been extensively studied in the last decades, atomization remains a key point in the understanding and modeling of cryogenic rocket engines combustion chambers because the physical processes in the chamber are highly dependent on the characteristics of the spray produced by the injector. The parameters describing the spray, like the expansion angle, the penetration depth, the droplet size distribution, are usually given as input data in the numerical simulation codes of such engines. To overcome this difficulty, ONERA is developing in the CEDRE code [8] a fully eulerian coupling strategy between "separated" and "dispersed" two-phase flows solvers. To reach this crucial challenge, diffuse interface models are used for primary atomization while kinetic models are used to compute the combustion of the spray. The aim is to compute the spray produced by a coaxial injector directly from the upstream global parameters (injection pressures, mass flow rates …) instead of imposing its characteristics as an input of the simulation.
In parallel to this numerical work, an experimental investigation was started on the Mascotte cryogenic test facility [9], in order to improve existing measurements, with the objective to provide relevant experimental data to validate the model. Experiments were run at 1 MPa in a single element combustion chamber. The injector was fed with liquid oxygen (LOX) atomized by a co-flow of gas at room temperature. Both cold flow and hot fire tests were achieved. The hydrogen used in the combustion tests was replaced by helium for the cold flow experiment. Similarity between cold and hot conditions was obtained by keeping constant the geometry, the chamber pressure, the LOX mass flow rate and the momentum flux ratio in the injector exit plane. The spray was investigated with a high speed camera in a backlighting optical configuration.
Keywords: cryogenic rocket engines, Modeling aspects, experimental investigations

1) Introduction

This paper comes within the scope of numerical simulations and experimental investigations for liquid-propellant rocket engines. In order to ensure the reliability of rocket engines, the best understanding of the different physical phenomena occurring in the combustion chamber has to be reached. In particular, the high frequency combustion instabilities which can lead to the destruction of liquid-propellant rocket engines have to be studied in a more comprehensive way. These complex instabilities result from the combination of multi-scales phenomena such as combustion, evaporation of oxygen droplets, turbulence and atomization. In this study we want to focus numerical simulations and experimental studies on the primary atomization which is expected to be deeply linked to the high frequency instabilities. CFD tools combined with experiments may thus help the development and enhancement of launcher propulsion systems.

In this paper, we focus on coaxial injection as depicted in Figure 1. The strong velocity difference between the two flow phases (LOX and Gaseous H_2) generates fluctuating accelerations. Due to these fluctuations, Rayleigh Taylor instabilities destabilize the liquid to create ligaments. These instabilities then grow and eventually provoke the peeling of the main LOX jet, which is referred to as "primary atomization". Large random-shaped liquid structures are thereby ejected towards the gas flow, subsequently undergoing "secondary break-up" when inertia forces exceed the liquid surface tension. This results in a spray of smaller LOX droplets, mainly spherical, which are dispersed by the turbulent gas flow, and finally vaporized to feed the combustion with hydrogen H_2. Such a configuration therefore exhibits a two-phase flow where the liquid phase is only composed of LOX, whereas the gas phase is made up with hydrogen H_2, vaporized oxygen O_2, and combustion products. Eventually, the resulting hot and high-pressure combustion products exhaust through a nozzle at supersonic speed, thereby providing the required thrust.

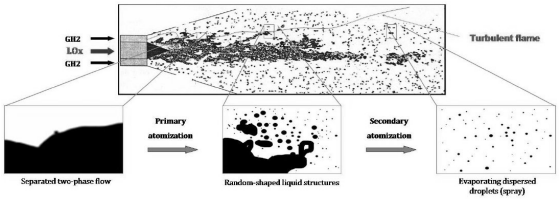

Fig 1 : Configuration of a combustion chamber within liquid-propellant rocket engines

Concerning numerical simulations, taking into account primary atomization seems to be possible if we consider the current computational resources. However, this type of simulations remains a tremendous challenge when considering primary atomization combined with the combustion of the small oxygen droplets conained in the spray. Indeed, the major issue is the wide range of scales to be considered and in this work we propose an original method coupling a fully Eulerian approach for "separated" and "dispersed" two phase flows.

Concerning the experimental investigations, the Mascotte test bench of Onera is an experimental facility for cryogenic combustion research. It is representative of a single element rocket engine injector. Interactions occurring between neighbour elements in actual combustion chambers, like the Vulcain 2 engine of the Ariane 5 launcher, where there are several hundreds of elements on the face plate, are therefore not taken into account, but they may be assumed negligible for the primary atomization phenomenon of interest in this paper. In this work, we deal with the difficulties to characterize liquid structures created during primary and secondary atomization of this high Reynolds and Weber number flow. The spray was investigated by means of a high speed camera in a backlighting optical configuration. Imaging is particularly adapted to study such sprays because it is less affected by high density gradients and non spherical liquid elements than laser based techniques. We also pay attention to compare in a qualitative way the differences of the spray between the inert and reactive cases. The droplet sizes were obtained by image analysis of the shadowgraphs [7].

At this time, the connexion between new numerical results and experimental investigations has not been reached. The main reason is that the numerical computations based on Large Eddy simulations are not yet converged. In the future, we intend to carry out the simulations and a quantitative comparison between numerical results and experimental investigations is our principal objective in order to validate the atomization model. Nevertheless, we want to point out that the simulations presented in this paper are very challenging and new for our knowledge.

2) Modeling aspects

As shown in Figure 1, the very major issue is actually the wide range of scales to be resolved in the successive atomization steps, up to the smaller spherical droplets of the spray. Following the classification proposed by Ishii [10], this kind of simulation exhibit a dense "separated" liquid phase near the injector as well as a "dispersed" liquid phase composed by oxygen droplets resulting from both primary atomization of the jet and secondary fragmentation of ligaments. In this work, we have selected a fully Eulerian approach coupling two solvers dedicated respectively to "separated" two-phase flows and "dispersed" two-phase flows. The "separated" two-phase flow will be described by interface diffuse models ranging from the seven equation model of Baer-Nunziato [11] to the four equations model i.e the multi-species Navier Stokes model. On the other hand, the "dispersed two-phase flow" will be described by a multi-fluid Eulerian model based on the kinetic Boltzmann approach [13]. In this study, we have chosen to couple the four equations LHF model (Locally Homogeneous Flow) with the sectional approach following the strategy previously proposed in [14] and working specifically on the atomization model. Other approaches [15]-[16] for propulsion and also for internal combustion engine have been proposed with for example Lagrangian description of the spray or Level Set and VOF method for the description of the dense liquid flow near the injector.

Before describing the two Eulerian solvers which have been used, we underline the principal key points of the numerical simulation:

a) Coupling Eulerian-Eulerian models for "separated" and "dispersed" two-phase flows into a Large Eddy Simulations (LES) approach involving combustion and turbulence.

b) Interface diffuse model for "separated" two-phase flow: a four equations LHF (Locally Homogeneous Flow) model, namely CHARME solver of the CEDRE software [8] including a liquid component for dense LOX and a multi-species gas for H_2 and burnt gases.

c) Kinetic model for "dispersed" two-phase flow : an Eulerian sectional approach, namely SPIREE [17] for oxygen droplets into the spray.

d) Classical but complex source terms between the two solvers as drag force and Abramzon-Sirignano Model [18] for heat and mass transfer of droplets.

e) Taking into account primary atomization between the solvers CHARME-SPIREE and also fragmentation inside the solver SPIREE

f) Finite volume method based on unstructured meshes with new MUSCL multi-slope technique [19].

The CHARME-solver for "separated" flow

In this solver, we consider a fluid mixture composed by one gaseous phase of n_g species and one liquid phase standing for the dense LOX. The classical Navier-Stokes system writes :

$$\frac{\partial \mathbf{Q}(\mathbf{U})}{\partial t} + \nabla \bullet \left[F_c(\mathbf{U}) - F(\mathbf{U}, \nabla \mathbf{U}) \right] = S(\mathbf{U})$$

In this system, conservative and primitive set of variables respectively write :

$$\mathbf{Q}(\mathbf{U}) = \left(\rho Y_1 \quad \dots \quad \rho Y_{ng} \quad \rho Y_l \quad \rho \mathbf{v} \quad \rho e_{tot} \right)^t$$

$$\mathbf{U}(\mathbf{Q}) = \left(P \quad T \quad \mathbf{v} \quad Y_1 \quad \dots \quad Y_{ng} \quad Y_l \right)^t$$

where $Y_i \quad i = 1, \dots, n_g$ stand for the mass fractions of gaseous species while Y_l stands for the mass fraction of the dense LOX. Then ρ is the mixture density, e_{tot} is the total energy and P, T stand respectively for the pressure and the temperature. The convective and diffusive fluxes can be written :

$$F_c(\mathbf{U}) = \mathbf{Q} \otimes \mathbf{v} + P(0 \quad \dots \quad 0 \quad \mathbf{I}_3 \quad \mathbf{v})^t$$

$$F(\mathbf{U}, \nabla \mathbf{U}) = \left(F_{\rho Y_1} \quad \dots \quad F_{\rho Y_{n_g}} \quad F_{\rho Y_l} \quad F_v \quad F_e \right)^t$$

We do not give more details on diffusion and convection. Then source term $S(\mathbf{U})$ will be described in the next section.

The SPIREE-solver for "dispersed" flow

Modeling of "dispersed" two-phase flows is based on a mesoscopic description of the dispersed phase. Particles are supposed to be spherical and fully characterized by a small set of variables: position $\mathbf{x}$, radius r, velocity $\mathbf{v}$ and temperature θ. In most applications, the particle number density function $f(t, \mathbf{x}, r, \mathbf{v}, \theta)$ contains all the necessary knowledge on the dispersed phase. By definition, $f(t, \mathbf{x}, r, \mathbf{v}, \theta) d\mathbf{x} dr d\mathbf{v} d\theta$ denotes the averaged number of droplets with a size in $[r, r + dr]$, a velocity in $[\mathbf{v}, \mathbf{v} + d\mathbf{v}]$, a temperature in $[\theta, \theta + d\theta]$ located in the volume $[\mathbf{x}, \mathbf{x} + d\mathbf{x}]$ at time t.

The following Boltzmann-like equation (introduced by Williams in [13]) expresses the conservation of the number density function f in the phase space:

$$\frac{\partial f}{\partial t} + \nabla_{\mathbf{x}} . (\mathbf{v} f) + \nabla_{\mathbf{v}} . (\mathbf{F} f) + \frac{\partial (Rf)}{\partial r} + \frac{\partial (Hf)}{\partial \theta} = \Gamma$$

In this balance equation, the left-hand-side stands for the “transport” of the particles in the phase space ($\mathbf{F}$, R and H respectively correspond to the force acting on a particle, the evaporation rate and the heat exchange rate) while Γ in the right-hand-side stands for the effect of fragmentation phenomena. Note that $\mathbf{F}$, R and H depend on the local gas composition, velocity and temperature.

Most of Eulerian approaches are based on the semi-kinetic model derived by taking different moments of the function f and integrating in the phase space over the variables velocity and temperature. So, if we define an averaged number of particles as well as an averaged velocity in the following way :

$$n(t, \mathbf{x}, r) = \iint_{\mathbf{v}, \theta} n(t, \mathbf{x}, r, \mathbf{v}, \theta) d\mathbf{v} d\theta$$

$$n(t, \mathbf{x}, r) \bar{\mathbf{v}}(t, \mathbf{x}, r) = \iint_{\mathbf{v}, \theta} \mathbf{v} f(t, \mathbf{x}, r, \mathbf{v}, \theta) d\mathbf{v} d\theta$$

Integrating the kinetic equation, and then using $f(t, \mathbf{x}, r, \mathbf{v}, \theta) \to 0 \quad \mathbf{v} \to -\infty, +\infty, \theta \to 0, +\infty$, we obtain the following equation for the averaged number :

$$\frac{\partial}{\partial t} n + \nabla_{\mathbf{x}} \left[n \bar{\mathbf{v}} \right] + \iint_{\mathbf{v}, \theta} \frac{\partial}{\partial r} (Rf) d\mathbf{v} d\theta = \iint_{\mathbf{v}, \theta} \Gamma d\mathbf{v} d\theta$$

As we want to precisely describe the polydispersion of the spray, models of order 2 in size are derived. So another equation for the mass conservation is introduced. Then equations for the conservation of momentum vector velocity and energy are also derived. As a consequence, the solver SPIREE writes :

$$\frac{\partial \mathbf{q}(\mathbf{u})}{\partial t} + \nabla \bullet \left[f_c(\mathbf{u}) \right] = s(\mathbf{u}) + \mathbf{\Gamma}$$

In this system of conservation laws, the conservative and primitive variables are :

$$\mathbf{q}(\mathbf{u}) = \left(\rho_d \quad \rho_d \mathbf{v}_d \quad \rho_d h_d \quad N_d \right)$$

$$\mathbf{u} = \left(D \quad \mathbf{v}_d \quad T_d \quad \alpha \right)$$

ρ_p stands for the particle density and N_d stands for the averaged number of particles by unit of volume. Then, h_d stands for the total energy and variables $D, \mathbf{v}_d, T_d, \alpha$ are respectively the particle diameter, the velocity, the temperature and the volume fraction. The convective flux is given by the following expression in which the pressure term is neglected

$$f_c(\mathbf{u}) = \mathbf{q} \otimes \mathbf{v}_d$$

The last step to get a fluid model for the particulate phase consists in eliminating the size variable r. The option, often called “multi-fluid” model or sectional model is chosen. It has been introduced in [12]. Information on droplets size distribution is kept at the macroscopic level thanks to a finite volume discretization with respect to the size variable. A set of equations is derived for each section and in this type of model, sections are coupled due to the finite volume approximation. Complex phenomena such as fragmentation can also be included.

Modeling classical source terms and turbulent combustion

The classical source terms between CHARME-SPIREE are $\mathbf{F}_D$, ϕ_C, $\dot{m}_{vap}$. These terms concern velocity relaxation as well as heat and mass transfer. The correlation of Schiller Naumann is used for the drag force and the Abramzon-Sirignano model [18] is used for the heat and mass transfer.

The H_2-O_2 combustion is then modelled using an infinitely fast chemistry assumption (high Damkohler number). This means that kinetics effects are not taken into account. The species production rates are related to the gap between the local concentration and the equilibrium concentration. In other words, the reacting species are relaxed towards chemical equilibrium with a finite relaxation time driven by a turbulent time scale. In the LES framework, such a time scale can be assumed from the resolved strain tensor. This approach is similar to the well-known “Eddy Break-Up” model as in both approaches infinitely fast chemistry is assumed. But fortunately, taking into account a local equilibrium involving radical species renders a much more accurate flame temperature. The reaction rate writes :

$$\dot{w}_i = cte\, \nu_{turb} \left(Y_{i,eq} - Y_i \right)$$

Now we describe the source terms $s(\mathbf{u})$ for each section of particles of SPIREE. The first component traduces the growth of mass due to primary atomization and its decrease by vaporization. If we now look at the source term $S(\mathbf{u})$ affected to the carrier phase CHARME. The first n_g components of gas species concern combustion and evaporation phenomena. The first term includes the evaporation of liquid oxygen droplets in the "dispersed" phase which creates gas oxygen in the carrier phase of CHARME. The component number $n_g + 1$ standing for the transport equation of mass liquid fraction concerns primary atomization. It transforms the dense LOX of CHARME into "dispersed" LOX in the appropriate sections of SPIREE.

$$s(\mathbf{u}) = \begin{pmatrix} s_{\rho_d} \\ s_{\rho_d \mathbf{v}_d} \\ s_{\rho_d h_d} \\ s_{N_d} \end{pmatrix} = \begin{pmatrix} \dot{M}_{ato} - N_d \dot{m}_{vap} \\ s_{\rho_d} \mathbf{v}_d + N_d \mathbf{F}_D \\ s_{\rho_d} h_d + N_d \left(\mathbf{F}_D . \mathbf{v}_d + \phi_c \right) \\ \dot{N}_{ato} \end{pmatrix}$$

$$S(\mathbf{U}) = \begin{pmatrix} S_{\rho Y_{O_2}} \\ S_{\rho Y_i} \\ \vdots \\ S_{\rho Y_{ng}} \\ S_{\rho Y_l} \\ S_v \\ S_e \end{pmatrix} = \begin{pmatrix} \dot{w}_{O_2} + N_d \dot{m}_{vap} \\ \dot{w}_i \\ \vdots \\ \dot{w}_{ng} \\ -\dot{M}_{ato} \\ -s_{\rho_d \mathbf{v}_d} \\ -s_{\rho_d h_d} \end{pmatrix}$$

Modeling secondary break-up

The general form of the fragmentation reads :

$$\Gamma(f)(\mathbf{v},r) = -\nu_{bup}(\mathbf{v},r) f(\mathbf{v},r) + \int_{\mathbf{R}^+}\int_{\mathbf{R}^3} \nu_{bup} h_{bup}(\mathbf{v},r,\mathbf{v}^*,r^*) f(\mathbf{v}^*,r^*) d\mathbf{v}^* dr^*$$

where $\nu_{bup}(\mathbf{v},r)$ denotes the breakup frequency. When $We > We_c$, the frequency is given by the following model with σ denoting the surface tension coefficient and τ_{bup} corresponding to the average break-up time :

$$\nu_{bup}(\mathbf{v},r) = \frac{1}{\tau_{bup}} \approx \frac{1}{5}\sqrt{\rho_g / \rho_p}\left\|\mathbf{v}_p - \mathbf{v}_g\right\|/(2r)$$

We refer to [21] for h_{bup} standing for the NDF of the droplets produced by the fragmentation of a given droplet of radius r^* and velocity $\mathbf{v}^*$. Then the experimental correlation for the Sauter Mean Diameter after fragmentation has been chosen following the work of Wert [22].

Modeling primary atomization

The model used to describe the mass transfer between solvers accounting for primary atomization reads in :

$$\dot{M}_{ato} = \rho Y_l \nu_{ato} \lambda_{ato}(Y_l)$$

where ρY_l is the liquid mass in a given volume of control, ν_{ato} is the characteristic frequency of the primary atomization process, and $\lambda_{ato}(Y_l)$ is an efficiency function. We assume the atomization frequency to be directly connected to the strength of the velocity gradient, which is the only information locally available in the LHF framework (no velocity difference is known). This could be estimated using several approaches, amongst which the Q criterion, the vorticity or the resolved strain tensor, all being based on the velocity gradient. In this study we have chosen to use the latter approach:

$$\nu_{turb} = \sqrt{2D^2}$$

$$D^2 = \sum_{ij} D_{ij} D_{ij} \quad ; \quad D_{ij} = \frac{1}{2}\left(\frac{\partial \bar{u}_i}{\partial x_j} + \frac{\partial \bar{u}_j}{\partial x_i}\right)$$

The efficiency function reads in:

$$\lambda_{ato}(Y_l) = 1 - \tanh(a_\lambda Y_l^{b_\lambda}) \quad a_\lambda = 4, b_\lambda = 2$$

It is designed to make sure that when some LOX mass is transferred from the fluid towards the spray in a given volume of control, the corresponding vanishing volume in the fluid is actually negligible. Otherwise the gas would experience some unphysical expansion in the volume control, which obviously has to be avoided, and the dispersed hypothesis made for the spray would not be respected. In other words, we use the numerical diffusion which spreads the interface over several mesh elements in order to carry out the mass transfer in a smooth way.

As this point with this model, the properties of the created droplets resulting from the primary atomization have to be assumed. They cannot be computed locally from resolved quantities as the LHF formalism provides too little information. Actually, these properties are estimated based on the instability analysis from Villermaux [20]. In the latter work, the drop size and velocity distributions of the spray are estimated as a function of the injected propellant properties (density ratio, inlet velocities, vorticity thickness...). Consequently, the knowledge of the steady operating conditions of the Mascotte configuration under study permits to derive an overall mean droplet diameter subsequent to the primary atomization process and a corresponding mean droplet velocity:

$$d_{ato} = 260\mu m \qquad \left\|v_{ato}\right\| = 16 ms^{-1}$$

The direction given to the droplet velocity in each mesh cell has been set to that of the fluid, which may be actually a rough approximation. Note that a very accurate and local value of the created droplet diameter is not of first order importance, as the use of a secondary break-up model is expected to rapidly modify and somehow correct the local droplet diameters. In fact, the zone of secondary atomization is expected to be correctly computed. Concerning the zone of primary atomization, the computation is limited by the LHF model in which only one velocity is available. In the future, we intend to improve the description of this zone using a 7 equations (2-velocities) model and to base the atomization model upon a local Weber number. Finally, the temperature of the created droplet is just set to the constant value which was used to describe the liquid phase in the fluid, namely 85 K, corresponding to the LOX injection temperature.

Preliminary results

In this section we present some preliminary numerical results obtained with the previously described coupling strategy. The 3D geometry is depicted on figure 2. The overall device is approximately 50 cm long, with a 50 mm wide section. The LOX post has a 5 mm diameter, whereas the total diameter of the injector (axial LOX + coaxial hydrogen) is 12 mm. We use a tetrahedral unstructured mesh made up with approximately 10M of elements. The mesh has been built so that the finest refinement is located near the injector exit, where atomization takes place. For the sake of simulation, the computational geometry has been split into 480 domains to allow parallel computing. The CPU time required for a simulation of 100µs physical time is about 4800 hours.

The figure 3 represents instantaneous fields of the following variables (starting from the top left-hand side and moving to the bottom right-hand side following the arrows):

- the LOX mass fraction in the fluid solver.

- the atomization source term, which shows where the LOX mass is transferred from the fluid solver to the spray solver.

- the total volume fraction of the spray (comprising all sections), which is only resulting from this mass transfer. Indeed, we started the computation with absolutely no droplets in the domain, and there is no droplets injected from boundary conditions either.

- the total vaporization rate which accounts for the inverse transfer: oxygen mass is leaving the spray solver to return to the fluid but under gaseous form due to the evaporation process.

- and this results in the gaseous oxygen field underneath.

- finally, as a result of the gaseous oxygen and hydrogen fields (bottom left-hand side), we get the water mass fraction and the temperature fields representing the combustion process (bottom right-hand side).

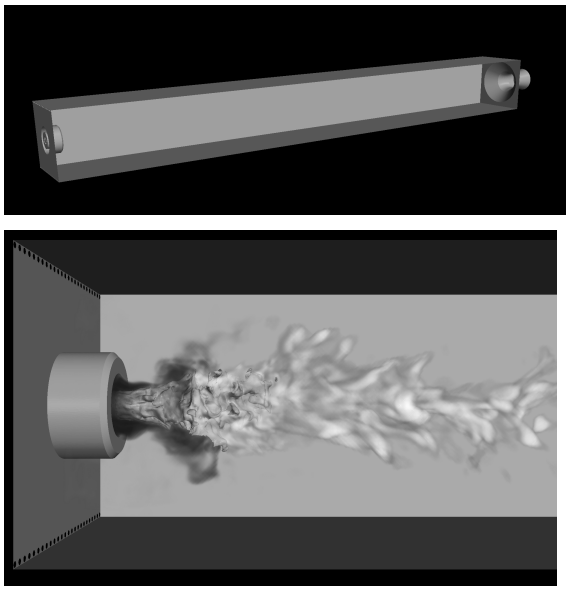

Fig 2 : representation of the complete chamber (top), and visualization of an instantaneous field near the injector (bottom)

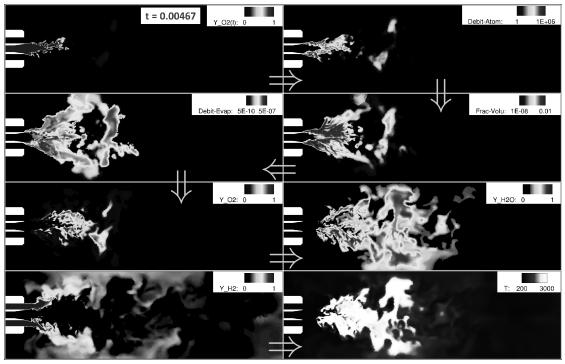

Fig 3 : preliminary results for the coupling between CHARME and SPIREE solvers taking into account for primary atomization in a cryogenic combustion chamber

3) Experimental investigations

We study the LOX spray in the atomization zone in order to validate the model described in the previous section. Experiments were conducted on the Mascotte test bench, located at Onera, Palaiseau center, which was designed for experimental studies of cryogenic propellants combustion. It provides data on elementary processes occurring in cryogenic jet flames such as atomization, vaporization and turbulent combustion, in conditions representative of actual rocket combustors. Several versions of the hardware have been

developed and manufactured for the different items of interest in experimental research (Habiballah et al. [3] and Candel et al. [4]). In the version used for the study reported here, a visualization module with two optical ports was placed near the injection plate. The combustion chamber had a square cross section of 50 mm side and was about 500 mm in length. A transition segment precedes the nozzle, to cross-connect the square combustion chamber to the axisymmetric nozzle. Ignition was provided by a gaseous oxygen / gaseous hydrogen torch igniter placed downstream of the windows. The combustion chamber was fed with liquid oxygen and an atomizing gas (hydrogen in the reacting case and helium in the cold flow simulation) through a single shear coaxial injector. The LOX post inner and outer diameters were d and 1.12d, respectively. The hydrogen sleeve outer diameter was 2.4d, as in the simulation described previously. In order to prevent the heating of the LOX during injection, the injection head was cooled by liquid nitrogen. Thus the LOX was injected at ~90 K while the gas was injected at room temperature. To protect the windows from hard thermal shocks, a film cooling of helium was injected with a mass flow rate of ≈6g/s.

Experiments were performed on the A-10 operating point, defined by the research group on "combustion in rocket engines", referenced in Candel et al. [4] and Habiballah et al. [3]. The chamber pressure was ≈1.0 MPa, the mixture ratio *ROF* was ≈2 and the momentum flux ratio J was ≈13 . Considering the oxygen critical pressure and temperature, LOX was injected in the combustion chamber in subcritical conditions.

	Fire test	Cold flow
Pc (MPa)	1.00	0.96
Tinj(LOX) (K)	89	90
Tinj(GH2) (K)	296	290
Re_d	62300	64300
ROF	2.4	1.7
J	12.99	12.38
We_G	26400	25300

Table 1: Main operating parameters during the steady-state conditions.

Table 1 summarizes the main parameters of cold flow and hot fire operating conditions. Those average values were computed over the whole set of test runs for this study. Comparison between the cold tests (H_2 line fed with He) and firing tests (H_2 line fed with H_2) seemed satisfactory in terms of relevant dimensionless numbers. The similarity between cold and reacting case was based on the following assumptions: the geometry of the chamber, the momentum flux ratio J, the chamber pressure *Pc* and the LOX mass flow rate were conserved. The gaseous Weber number We_G was ~25000 and ~26000 for the cold and reacting cases respectively. The liquid Reynolds number Re_d based on the LOX post diameter d was ~63000 for both cases. According to the classification, proposed by Lasheras and Hopfinger [5], for the coaxial jet breakup regimes as a function of the three parameters We_G, Re_d and J, the jet lies in a fibre-type regime, where the atomization is driven by the atomizing gas velocity, i.e. the velocity in the outer ring of the coaxial injector. The relative motion with respect to the atomizing gas causes an instability of the liquid stream and a tendency to form waves that grow rapidly in amplitude to the point where they break down into large liquid structures, droplets and ligaments (Vingert et al. [6]). Typical pressure and flowrate traces are shown on Figure 4. Each run had a steady state period of at least 12 s for the reactive conditions and 20 s for the cold flow tests (not shown here), largely sufficient to record three short periods with the high speed camera. Vertical dashed lines show the beginning of these recording periods of ≈0.5s each. 14 hot runs and 21 cold flow tests were conducted to obtain a complete map of the spray

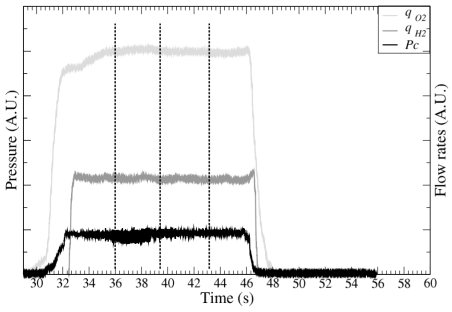

Figure 4: Typical pressure and flow rates signals of a hot fire test. Vertical dash lines indicate the beginning of the recording periods.

The spray produced by the coaxial injector in these conditions was already investigated by. Gicquel and Vingert [1] with a Phase Doppler

Particle Analyser (PDPA), but the atomization zone was not deeply investigated because of a low validation rate on size measurements. Indeed, in this region where lots of liquid elements are not spherical, Phase Doppler systems have difficulties to measure these droplet sizes with confidence. Moreover, Rousset et al. [2] pointed out that the optical setup of a Phase Doppler system needs some cautions to be applied on cryogenic two phase flows, mainly because of the relative refractive index variations of the medium due to the high temperature gradient between the flame and the cryogenic fluid. Imaging techniques may therefore be more suited to perform drop-size measurements in those conditions, because they are less affected by the non spherical shape of the liquid structures and they are less sensible to index variations. The use of high speed cameras can provide also information on the droplet velocities.

The spray was enlightened in a backlight configuration by a high magnitude light source Prolight 575W, providing a white incoherent and continuous light. A Fresnel lens and a transparent sheet were placed in front of the light to ensure a homogeneous background on images. Images of the spray were recorded with a Phantom v711 high-speed camera. This camera is composed of a 12-bit CMOS sensor of 1280 x 800 square pixels of 20 µm side. The size of the sensor is directly related to the frequency rate. We used three partitions of the memory, each one with its own frame rate/sensor size setup, starting at the times shown by vertical dashed lines on Figure 4. An objective of 105 mm focal length was mounted on the camera and the aperture was fixed to f/5.6 during the whole test series. The exposure time of the camera was fixed at its minimum to 1µs to freeze the droplets on images. It can induce a pixel shift on droplet images, due to the droplet velocities, which was estimated at ¼ of a pixel in the reacting conditions. The optical setup was kept the same for cold and hot fire tests. To cover the whole window, whose length is ~15*d*, the camera was moved in a vertical focus plane (x,y) with small fields of view of 2*d* x 2*d*. The *x* axis is considered as the injection axis. The small size images were assembled on Figure 5, the more rigorously possible, to compare the reacting and the cold jet at the same scale. For the reacting case only, we define four 512 x 512 pixel regions of interest (ROI): A, B, C, D, shown on figure 5, which were used to perform drop-sizing measurements. Those ROI have been chosen off-axis, focused on the secondary atomization zone, where the optical density of the spray was not too high so that we could characterize droplets individually and perform image processing methods.

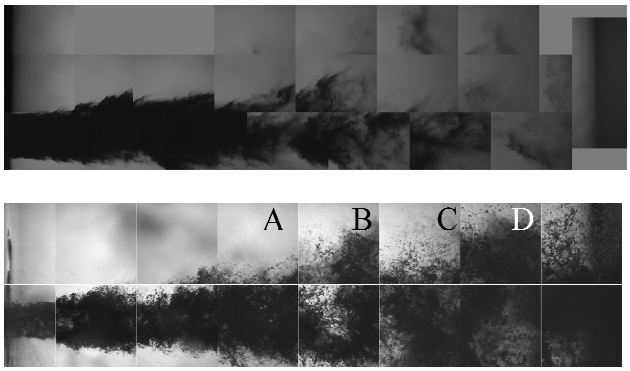

Figure 5: Instantaneous images of the spray in cold flow (top) and reacting conditions (bottom). Field of view: 15*d* x 4*d*.

Cold/hot flow comparison

The morphology of the jet at the injector exit is shown in Figure 6: the cold flow (LOX with gaseous He, bottom) and the reacting flow (LOX with gaseous H_2, top) can be qualitatively compared. For each case, a couple of successive images (1280 x 800) are shown, recorded at 7.5 kHz with the same optical setup. The LOX post exit of the injector is located on the left edge of the images. The fibre-type break-up regime is characterized by the creation of very thin and short liquid fibers created as soon as the continuous liquid jet exits from the nozzle. These fibres are rapidly peeled off the jet, stretched by the differential velocity between the liquid jet and the outer gas stream. Due to this stretching, the liquid jet is highly modified and disintegrates into liquid filaments which, in turn, are broken, creating droplets. The characteristic break-up time is very short, which means a rapid atomization of the majority of the liquid. The droplets are produced in very small sizes, several orders of magnitude smaller than the diameter of the injector

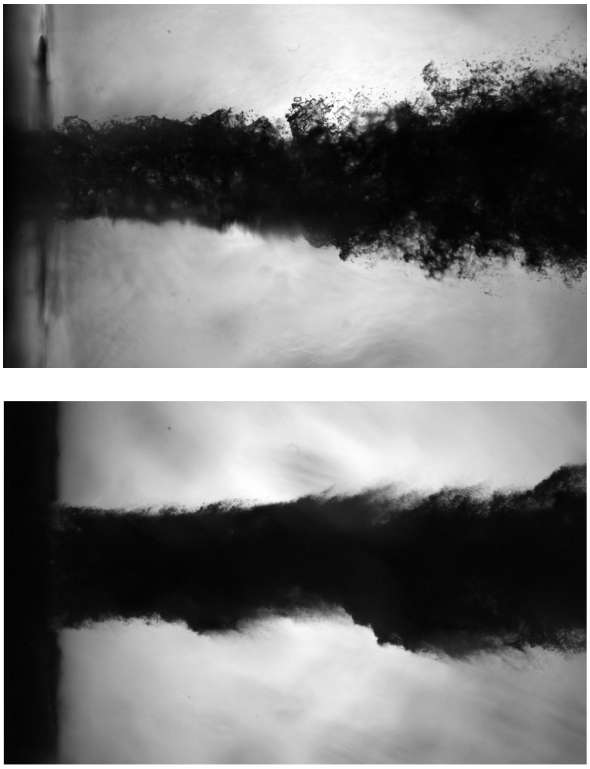

Figure 6: Comparison between reacting (top) and cold (bottom) flows. Images (1280 x 800) were recorded at 7.5 kHz. Field of view: 5.1*d* x 3.2*d* .

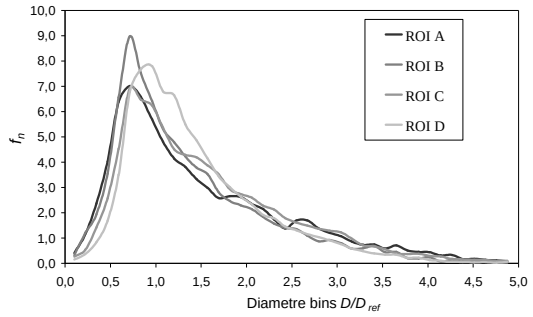

Figure 7: Drop size distribution evolution towards the injection axis in ROI A to D. Reacting case.

The probability density function (pdf) were obtained by image processing [7] of the shadowgraphs. The pdf of the spray in ROI A to D is shown on Figure 7, in the reacting case only. The pdf exhibits a large shape with a slow decrease towards the biggest diameters. The drop size distribution seems to be translated towards the biggest diameter as the axial distance from the injector increases. This evolution, often observed in burning sprays studies is probably due to the evaporation of the droplets induced by combustion. The smallest drops (D/D_{ref} *<1.0*) evaporate much more rapidly than large droplets (D/D_{ref}*>1.5*) even if the D^2 law alone is not applicable in such turbulent flames.

4) Conclusions

In this work we have presented numerical simulations and experimental investigations for liquid-propellant rocket engines. The numerical strategy is based on two Eulerian solvers in order to take into account for the crucial problem which is the primary atomization. The preliminary results seem to be very promising and allow to validate the strategy. In the future, we intend to converge the actual large eddy simulations and as well to increase the level of resolution in term of meshes moving to high performance computing. These first results allow us to validate the strategy of the coupling using two Eulerian solvers. The next step to be reached is to converge the Large Eddy Simulation and to compare the results with experimental investigations. Then we intend to use a 7 equation 2 velocities model to improve the atomization model according to experimental investigations.

In the other hand the experimental investigations provides parameters to describe the atomization as for example the velocity or droplet sizes. With the use of the 7-equation model, we intend in the future to compare in a quantitative way numerical and experimental results. The goal to reach is to validate and perform the atomization model which would be based on two different velocities for gas and liquid. Global parameters such as expansion angle, penetration depth or the mean size of droplets will be used to calibrate velocities relaxation as well as parameters of the atomization model.

5) Bibliography

[1] GICQUEL, P. and VINGERT, L., Flow investigations of cryogenic sprays in combustion at sub and supercritical conditions, *16th Annual Conference in Liquid Atomization and Spray Systems*, Darmstadt, Germany, 2000.

[2] ROUSSET, B., CHATAIN, D., PUECH, L, THIBAULT, P., VIARGUES, F., and WOLF, P.-E., Visualization in cryogenic environment: Application to two-phase studies, *Cryogenics*, Volume 49, Issue 10, Pages 554-564, 2009.

[3] HABIBALLAH, M., Orain, M., Grisch, F., VINGERT, L., and GICQUEL, P., Experimental studies of high-pressure cryogenic flames on the Mascotte facility, *Combustion Science and Technology*, vol.178, pp. 101-128, 2006.

[4] CANDEL, S., JUNIPER, M., SINGLA, G., SCOUFLAIRE, P. and ROLON, C., Structure and dynamics of cryogenic flames at supercritical pressure, *Combustion Science and Technology*, vol.178, pp. 161-192, 2006.

[5] LASHERAS, J.C. and HOPFINGER, E.J., Liquid jet instability and atomisation in a coaxial gas stream, *Annual Review of Fluid Mechanics*, vol.32, pp.275-308, 2000.

[6] VINGERT, L., GICQUEL, P., LOURME, D., and MENORET, L., Coaxial Injector Atomization, *Liquid Rocket Engine Combustion Instability*, *Progress in Aeronautics and Astronautics*, AIAA Inc., pp.145-189, 1995.

[7] FDIDA, N., BLAISOT, J.B., FLOCH, A. and DECHAUME, D., Drop-size measurement technique applied to gasoline sprays, *Atomization and sprays*, vol.20, number 2, pp.141-162, 2010.

[8] A. REFLOCH et al - *CEDRE Software*. THE ONERA JOURNAL AerospaceLab, Issue 2, CFD Platforms and Coupling, 2011.

[9] L. VINGERT, M. HABIBALLAH, J.C. TRAINEAU. *MASCOTTE : a research facility for high pressure combustion of cryogenic propellants.* In 12th European Aerospace Conference, Paris, 1999

[10] M. ISHII - *Thermo-Fluid Dynamic Theory of Two-phase flow*. Volume 22 of Direction des etudes et recherches d'électricité de France. Eyrolles, Paris, 1975.

[11] M.R. BAER, J.W. NUNZIATO. *A two-phase mixture theory for the deflagration-to-detonation transition (DDT) in reactive granular materials.* Journal of Multiphase flows, 12 : 861-889, 1986.

[12] J.B. GREENBERG, I. SILVERMAN, Y. TAMBOUR - *On the Origins of Spray Sectional Conservation Equations.* Combustion and flame 93, pp. 90-96, 1993.

[13] F.A. WILLIAMS. *Combustion Theory* (Combustion Science and Engineering Series). Ed F A Williams, Reading, MA, Addison-Wesley, 1985.

[14] C. LE TOUZE, A. MURRONE, E. MONTREUIL. *Numerical coupling strategies for the "separated-to-dispersed" transition within the liquid phase of cryogenic rocket engines.* 5TH EUCASS, 2013.

[15] R. LEBAS T. MENARD, P.A. BEAU, A. BERLEMONT, F.X. DEMOULIN. *Numerical simulation of primary break-up and atomization : DNS and modelling study.* International Journal of Multiphase flow. 35, pp 247-260, 2009

[16] A. VALLET, A. BURLUKA, R. BORGHI. *Development of a Eulerian model for the atomization of a liquid jet.* Atomization and Sprays, vol 11, pp 619-642, 2001

[17] A. MURRONE, P. VILLEDIEU. Numerical Modeling of Dispersed Two-Phase Flows. THE ONERA JOURNAL AerospaceLab, Issue 2, CFD Platforms and Coupling, 2011.

[18] B. ABRAMZON, W.A. SIRIGNANO - *Droplet vaporization model for spray combustion calculations.* International Journal of Heat and Mass Transfer, Vol. 32, n°9, pp. 160-1618, 1989.

[19] C. LE TOUZE, A. MURRONE, H. GUILLARD. *Multislope MUSCL method for general unstructured meshes.* Submitted to Journal of computational Physics, 2014.

[20] P. MARMOTTANT, E. VILLERMAUX. *On spray formation.* JFM 498, p 73-112, 2004

[21] P.J. O'ROURKE and A. AMSDEN - *The TAB method for numerical calculation of spray droplet breakup.* Technical Report, Los Alamos National Laboratory, New Mexico, (1987). 87545.

[22] K.L. WERT - *A rationally-based correlation of mean fragment size for drop secondary breakup*. International Journal of Multiphase Flow, 21(6) :1063–1071, (1995).